

Reforestation analysis using temporal NDVI and ALOS-2 PALSAR-2 polarimetric data

Irina I. Kirbizhekova¹, Tumen N. Chimitdorzhiev¹, Arkady K. Baltukhaev¹,
Aleksey V. Dmitriev¹ and Pavel N. Dagurov¹

¹*Institute of Physical Materials Science, Ulan-Ude, Russia*

Abstract

The article presents the results of assessing the restoration of a pine forest on a test site in the vicinity of Ulan-Ude after the 2003 fire and reforestation work. The studies were carried out on the basis of the full polarimetric information of the L-band ALOS-2 PALSAR-2 from 2017–2019. and NDVI indices based on the optical range of Resurs-P and Landsat 1995–2021. The results of the polarimetric decomposition of the $H - A - \alpha$ -classification indicate significant differences between the test and reference forest areas. Studies of long-term seasonal fluctuations of the NDVI for the test site revealed differences in the rate of recovery of multi-seasonal tracks to the pre-fire level and the level of the reference forest areas.

Keywords

Radar polarimetry, Cloude – Pottier decomposition, Landsat, NDVI, reforestation.

1. Introduction

Currently, the protection, conservation and restoration of forests in the Russian Federation are becoming priority areas of forestry activities. Within the framework of the federal program “Preservation of Forests” of the national project “Ecology” it is planned to achieve a full balance of forest destruction and restoration by 2024, up to 1.5 million hectares per year [1]. In these conditions, research and development of effective, low-cost methods of control and monitoring of the reforestation process in huge, often inaccessible territories are relevant. In this connection, it became necessary to create a technology for remote sensing to solve the set tasks [2, 3]. Research in this area is rare and fragmentary. It is not yet possible to completely replace land-based forest survey methods with remote ones.


Remote methods for studying reforestation processes can be classified according to the type of sensors (passive and active); by the range of electromagnetic radiation (optical, radar); by the area of variability of the information used (spectral, texture, polarimetric, seasonal and long-term time series). A separate group is made up of methods that combine information from different ranges from different satellites. A detailed overview of various methods for monitoring boreal forest regeneration is provided in [4]. The most simple and widespread methods are those using tracks of vegetation indices, their differences and ratios, both in relation to pre-fire values and values for control areas of healthy forest.

SDM-2021: All-Russian conference, August 24–27, 2021, Novosibirsk, Russia

✉ kirbizhekiova@bk.ru (I. I. Kirbizhekova)



© 2021 Copyright for this paper by its authors. Use permitted under Creative Commons License Attribution 4.0 International (CC BY 4.0).

 CEUR Workshop Proceedings (CEUR-WS.org)

In the Republic of Buryatia (RB), forest loss is associated mainly with forest fires and felling. Forests cover 29.806 million hectares or 84.8% of the territory. About 75% of RB forests belong to classes I–III, the most fire hazardous [5, 6]. On average, 940–1000 fires occur per year, covering an area of 74.6–76.8 thousand hectares. The main factors of forest fire hazard are the predominance of conifers, climate aridity and the human factor [7, 8, 9]. The species composition is heterogeneous throughout the territory of the RB, but in general, the main breed-forming species are Siberian larch and Gmelin larch – 53.5%, Scotch pine – 19.5%, cedar – 14.5%. Winters with little snow, lack of precipitation in spring and in the first half of summer significantly increase the risk of forest fires. The most common cause of fire is human activity and carelessness. According to statistics, up to 81.3% of forest fires occur precisely through human fault, near settlements or roads [6, 7]. In remote, hard-to-reach places, fires occur much less frequently. But the burning area is usually larger due to remoteness, inaccessibility, and limited fire extinguishing capabilities for ground services. The direct economic damage from forest fires is growing every year, reaching a record 35 billion rubles in 2015, or 17% of the gross regional product of the Republic of Buryatia [9]. It is more difficult to assess the damage from disturbance and disappearance of local ecosystems. On a more global level, colossal damage is inflicted on the unique ecosystem of Lake Baikal.

When carrying out reforestation in the RB, the main role is assigned to the natural method. With clear felling, undergrowth remains, which can account for up to 60% of the area of mature and over-mature stands. On burnt-out areas, measures are taken to promote natural regeneration: preservation of undergrowth, soil mineralization, care for self-seeding and undergrowth. Artificial forest reforestation is on average 6.9% of the total volume of reforestation work, including 5.9% for fries [10]. It is carried out by planting Scots pine seedlings. For the period 2005–2016 plantings were carried out on an area of 23.153 thousand hectares. Until 2005, sowing was also carried out. The survival rate of young seedlings and seedlings varies from 25 to 85% depending on the location and growing conditions, planting technology and subsequent care [10].

This article presents the results of applying the full polarimetric information of the L-band ALOS-2 PALSAR-2 2017–2019. to assess the success of the pine forest restoration process after a forest fire in 2003. The degree of forest restoration was also estimated based on changes in seasonal NDVI values according to Landsat 1995–2021 data.

2. Object and territory of the study, satellite data

The test site of a pine forest with an area of 68.8 hectares is located north of Ulan-Ude, in the spurs of the Ulan_Burgasy ridge. Geographic coordinates: 107.64 °N, 51.90 °E The relief is mountainous, with heights from 680 to 800 m, slopes up to 30°. After a forest fire in the spring of 2003, reforestation and planting of Scots pine seedlings were carried out in the lowlands and on gentle slopes. The rest of the territory is undergoing natural forest regeneration. For comparison, polarimetric characteristics and NDVI were also investigated in the following areas: 1) pine forest; 2) mixed forest (birch, aspen, pine, etc.); 3) a field without vegetation (for 2021) and 4) dacha non-profit partnership “Lesnoye”.

The area of the sites is 21.2, 8.7, 14.2 and 9.8 hectares. The surface of these sites is flatter, with

elevation differences up to 30–50 m and slopes up to 5–10°. Figure 1 shows the location, the layout of the plots, photographs of the forest and undergrowth unaffected by the fire. The age of young animals varies from 3–4 to 15 years, the height does not exceed 4 m.

In the study area, the climate is temperate, sharply continental, arid. The average annual air temperature is -0.1°C . Average monthly temperatures range from -23.3°C in January to $+19.8^{\circ}\text{C}$ in July. Average precipitation is 265 mm/year of precipitation, mainly in summer. This area is characterized by a high level of solar radiation, the annual number of hours with the sun is more than 2400 hours.

The following satellite data were used to determine the polarimetric characteristics and NDVI:

- L-band radar data with full polarization (hh, hv, vh, vv) ALOS-2 PALSAR-2 dated April 05, 2017, April 18, 2018 and August 30, 2019;
- multispectral data of Resurs-P KShMSA dated March 04, 2018 with a resolution of 1.795 m;
- NDVI time series averaged over 32-day intervals according to Landsat-5 data from 01/01/1995 to 16/10/2011 and Landsat-8 from 07/04/2013 to 06/03/2021 [11].



Figure 1: a — the location of the test site; b — layout of test and control sections; c — a photo of a forest unaffected by the fire; d — photo of pine undergrowth.

3. Decomposition and classification of polarimetric data

The theoretical foundations of radar polarimetry methods are well known [12, 13, 14]. Radar images are a set of second-order scattering matrices S , which characterize the reflected pulse in four polarization channels with matched (hh, vv) and transverse (hv, vh) orientations of the emitter and receiver. The complex elements of the scattering matrix S contain amplitude and phase information for each of the four polarization channels. Direct interpretation of matrix elements is difficult. Therefore, methods have been developed for decomposition or decomposition of the scattering matrix into components with a simpler interpretation. One of the most common methods is the Cloude – Pottier decomposition [12, 13, 14]. The Cloude – Pottier method allows one to identify up to 16 classes of the process of polarized wave scattering on objects on the Earth’s surface. S is split into three components: entropy H , anisotropy A and parameter α . The first parameter characterizes the degree of statistical disorder. The second is the ratio of the dominant and minor eigenvalues of the coherence matrix. The third is the dominant scattering mechanism, expressed in angular measure in the range from 0 to 90°. At values of α close to 0°, scattering from the surface of flat areas of the earth dominates. At average values of $\sim 45^\circ$, the volumetric scattering mechanism, characteristic of vegetation, prevails. At values of the parameter α close to 90°, the greatest contribution to the reflected signal is made by double and multiple reflections, which are mainly typical for settlements, for trunks and large branches of trees, stepped terrain, etc. Thus, the set of parameters H , A , α means a well-defined composition, combination and weights of the main and non-main scattering mechanisms for each object, making it possible to assign it to one of 16 classes. Based on data from ALOS-2 PALSAR-2 2017–2019. polarimetric decomposition into $H - A - \alpha$ components was carried out. Figure 2 shows a fragment of the Pauli decomposition RGB image. The figure shows in color the main types of scattering over the study area in 2018. Green corresponds to volumetric scatter from vegetation, blue to surface scatter on relatively flat and smooth areas, and red to multiple scattering for buildings, trunks and large tree branches. At the time of the survey (2018), the nature of the scattering of the polarized radar wave at the research site differs from the scattering in the neighboring areas of a healthy forest, a field without vegetation, and a summer cottage village. The area is dominated by blue color with a slight touch of green and red, which corresponds to the dominance of the surface type of scattering. A small proportion of volumetric and multiple types of scattering indicates a weak presence of vegetation, i.e. one of the initial stages of reforestation.

Table 1 shows the average values of the parameters $H - A - \alpha$ and their standard deviations for all polygons. For pine and mixed forests, the indicators are close, so they are combined into one group. In accordance with the values of the parameters, it is possible to characterize the scattering processes and their changes. For example, judging by the low values of the parameter $\alpha = 20 - 35^\circ$, the surface type of scattering dominates in the fields and young growth. Average entropy $H = 0.55 - 0.68$ is evidence of surface roughness, except for the low value of the field entropy in August $H = 0.44$, i.e., it becomes smoother and smoother. The lower anisotropy of young animals (0.38–0.46) indicates the presence of other types of scattering besides surface, while the anisotropy of the field (0.50–0.51) indicates the predominance of one type of scattering and a weaker presence of other types.

The last row of the table contains the Fractional Vegetation Cover (FVC) values calculated from

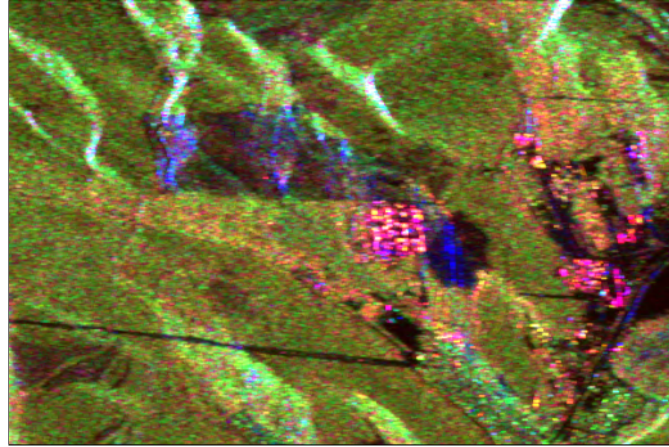


Figure 2: Fragments of RGB-images Pauli decomposition according to ALOS-2 PALSAR-2 data dated April 18, 2018.

Table 1

Statistical indicators of the parameters $H - A - \alpha$ (mean \pm stdv) for 2017–2019.

Sites	Entropy H			Anisotropy A			Parameter α		
	05.04.2017	18.04.2018	30.08.2019	05.04.2017	18.04.2018	30.08.2019	05.04.2017	18.04.2018	30.08.2019
Field	0.55 \pm 0.16	0.60 \pm 0.18	0.44 \pm 0.19	0.52 \pm 0.12	0.50 \pm 0.13	0.51 \pm 0.13	27.0 \pm 9.9	30.0 \pm 10.1	20.3 \pm 10.8
Undergrowth	0.58 \pm 0.14	0.68 \pm 0.12	0.65 \pm 0.14	0.46 \pm 0.13	0.40 \pm 0.13	0.38 \pm 0.12	29.5 \pm 9.2	35.1 \pm 8.7	32.0 \pm 9.1
Forest	0.79 \pm 0.10	0.84 \pm 0.07	0.84 \pm 0.07	0.35 \pm 0.12	0.31 \pm 0.10	0.31 \pm 0.10	50.6 \pm 5.5	51.3 \pm 6.1	49.5 \pm 5.74
DNP Lesnoe	0.49 \pm 0.16	0.48 \pm 0.18	0.53 \pm 0.14	0.76 \pm 0.14	0.74 \pm 0.15	0.76 \pm 0.15	49.0 \pm 13.9	50.9 \pm 13.9	47.2 \pm 12.82
fvcP, %	13	33	53	35	53	65	8	24	41
FVC_32d (L8)	24	29	97	—	—	—	—	—	—

the NDVI_32d Landsat-8 data for April 2017, April 2018 and August 2019 using the formula [15]:

$$\text{FVC} = \frac{\text{NDVI}_{\text{test}} - \text{NDVI}_{\text{soil}}}{\text{NDVI}_{\text{pine}} - \text{NDVI}_{\text{soil}}} \cdot 100\%, \quad (1)$$

where $\text{NDVI}_{\text{test}}$, $\text{NDVI}_{\text{soil}}$, $\text{NDVI}_{\text{pine}}$ — are the average values of the index for the test area of pine undergrowth, the area of the field without vegetation, and the control area of the pine forest. To assess the degree of similarity between the polarimetric indices H , A , $\alpha(P)$ of the test and control sections, we introduce a similar index fvcP by the formula:

$$\text{fvcP} = \frac{P_{\text{test}} - P_{\text{soil}}}{P_{\text{forest}} - P_{\text{soil}}} \cdot 100\%. \quad (2)$$

where P_{test} , P_{soil} , P_{forest} — average values of polarimetric parameters H , A , α for the test plot of pine undergrowth, a plot of a field without vegetation, and a control plot of pine and mixed forest. The fvcP values characterize the similarity or difference between the parameters of the test plot of pine undergrowth with the parameters of open soil (0%) and the reference forest (100%). The calculated fvcP values are shown in the penultimate line.

These values are a measure of the approximation of the corresponding parameters to the characteristics of the control samples, expressed in %. In the case of NDVI, the benchmark is pine forest, in the case of parameters $H - A - \alpha$ — pine and mixed forest. As you can see from the table, the values of all indices increase from 2017 to 2019. In the spring period (April 2017 and 2018), the polarimetric parameters and NDVI of undergrowth are closer to the characteristics of the field (fvcP = 8 – 35% and FVC = 24 – 29%), except for anisotropy (fvcA = 53%). In August 2019, the entropy (fvcH = 53%), anisotropy (fvcA = 65%), and NDVI (FVC = 97%) of the test site approach the corresponding forest indicators. In the first case, the entropy did not increase, but, on the contrary, decreased from 0.68 to 0.65, while the entropy of the forest did not change (0.84). Thus, the shift of the fvcH index from 33% to 53% is caused by a decrease in the entropy of the field from 0.60 to 0.44 due to a change in its state. In the second case, there is a real approximation of the anisotropy of the test section (0.38) to the indicator of the control section 0.31, i.e. in the summer season, the role of secondary types of scattering (volume and multiple scattering) increases. In the latter case, an increase in the NDVI index to 97% in August in the study area is justified and associated with the peak of the growing season. The fvc α index increased significantly in August, but the growth is relative to a decrease in the α parameter for the field. The dominant type of scattering remains unchanged.

$H - \alpha - A$ -classification showed significant differences in the distribution of various mechanisms of scattering of the radar pulse. The distribution of the classes of the test plot is more similar to the distribution of the classes for the field. The share of the territory dominated by volumetric scattering characterizing the thickness and density of the forest environment, averaged over three years, is 77.7% for the forest and 21.3% for the young. For multiple scattering, which characterizes the mass of trunks and thick branches, 19% and 0.2%, respectively. The proportion of surface scattering characterizing relatively open and flat areas is 3.4% and 78.5%, respectively.

4. Distribution of young pine trees according to high-resolution optical data

For comparison with the results of polarimetry, a mask of coniferous vegetation was created based on an early spring high-resolution optical image. For this, the NDVI was calculated using the Resurs-P image dated April 03, 2018 with a spatial resolution of 1.795 m. Statistics showed that for the control plot the average NDVI value is 0.251, the standard deviation is 0.020, for 98.56% of the NDVI area > 0.2 . For the test site, the same indicators are 0.1920, 0.0324 and 38.06%. According to ALOS-2 PALSAR-2 data dated April 18, 2018, volumetric scattering is dominant on 76.46% of the forest area and 31.1% of the test area. This is significantly lower than the estimates of vegetation obtained from the data of the optical range. Figure 3 shows a fragment of the NDVI image with the contours of the study areas in gray and a mask of young

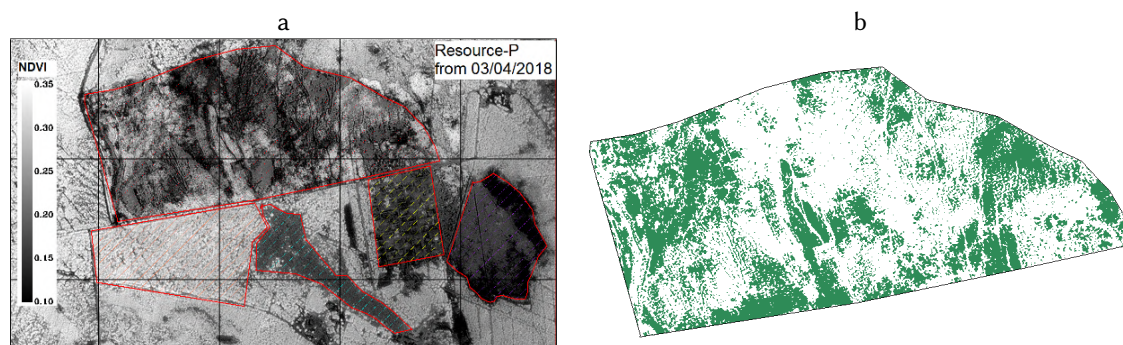


Figure 3: Pine distribution according to Resurs-P data dated 03/04/2018 with a resolution of 1.795 m: a — NDVI image; b — young stock mask ($\text{NDVI} > 0.2$).

pine for the test site, built taking into account the threshold value $\text{NDVI} = 0.2$. Obviously, with this approach, only dense islets of young pine stands with a high degree of crown closure are taken into account. To account for sparse undergrowth or detached trees with insufficiently large crowns, images with a higher resolution are required.

5. Seasonal and perennial NDVI changes

To assess the reforestation process in the test and control plots, seasonal and long-term changes in the NDVI (Normalized Difference Vegetation Index) were studied. The NDVI indices for each of the sites are calculated directly on the Earth Engine Data Catalog site [12].

The data of the Landsat-5 and Landsat-8 red and near infrared channels averaged over 32-day intervals are used. Small gaps in the time series are due to cloudiness and the gap between the Landsat-5 and Landsat-8 surveys. Variations in values are seasonal. The maximum values are in summer time, the minimum in winter. Some of the fluctuations are associated with high cloudiness of values, while even at the peak of the growing season, the NDVI values may decrease to zero.

As can be seen from the graphs before the 2003 forest fire, the profiles practically coincide. The correlation coefficient of the two series for 1995–2002 is 0.97, which is evidence of a high degree of similarity between the burnt pine forest in the test plot and the pine forest in the control plot. In 2003, after a fire in the test area, there is a sharp drop in the index and a slow growth in subsequent years. Figure 4, a shows a graph of the relative reforestation index RRI (Relative Regrowth Index), calculated according to the following formula [13]:

$$\text{RRI}(t) = \text{NDVI}_{\text{test}}(t) - \text{NDVI}_{\text{pine}}(t), \quad (3)$$

where $\text{NDVI}_{\text{test}}$ — the average value of the index over the territory of the test site, $\text{NDVI}_{\text{pine}}$ — control plot of pine forest. As can be seen from the figure, the differences in the test and control sections before the fire are insignificant. After a fire, the amplitude of seasonal variations in the RRI index increases tens of times. In the first 5 years after the fire, the changes are insignificant, then a slow decay is observed, which indicates the beginning of forest restoration.

The restoration of boreal forests after fires goes through several stages. First, the grass cover is restored, then the secondary species, and finally the main conifers. Full natural reforestation can take up to 80–100 years; the process is more dynamic when carrying out forest management works. To assess the degree of recovery, the seasonal average values of the NDVI index were calculated. Figure 4, b shows graphs of moving averages NDVI_32d for four climatic seasons of the Baikal region: winter (November–December–January–February–March), spring (April–May), summer (June–July–August) and autumn (September–October). The graphs show different recovery rates to pre-fire levels. The rapid growth in the first 2–3 years of the summer NDVI is consistent with the recovery of the herbaceous community. Average growth over the first 10 years of the spring and fall NDVI indicates recovery of shrubs and deciduous plants. Lack of growth for 7 years after the fire and further slow growth of winter NDVIs indicate the beginning of pine recovery.

To assess the degree of forest restoration, the Stand Regrowth Index (SRI) was calculated using the following formula [16]:

$$\text{SRI}(t) = \frac{\text{NDVI}(t)}{\text{mean}(\text{NDVI}_{\text{before}})} \cdot 100\%, \quad (4)$$

$$\text{SRI}(t) = \frac{\text{NDVI}(t)}{\text{max}(\text{NDVI}_{\text{before}})} \cdot 100\%. \quad (5)$$

Average and maximum pre-fire values $\text{mean}(\text{NDVI}_{\text{before}})$ and $\text{max}(\text{NDVI}_{\text{before}})$ are calculated for the time interval 1995–2002. Figure 5 shows the seasonal graphs of the SRI indices for two periods of 2004–2011 and 2013–2021. The calculation results for the averaged NDVI values are shown on the graph with solid lines, for the maximum values at each time interval –

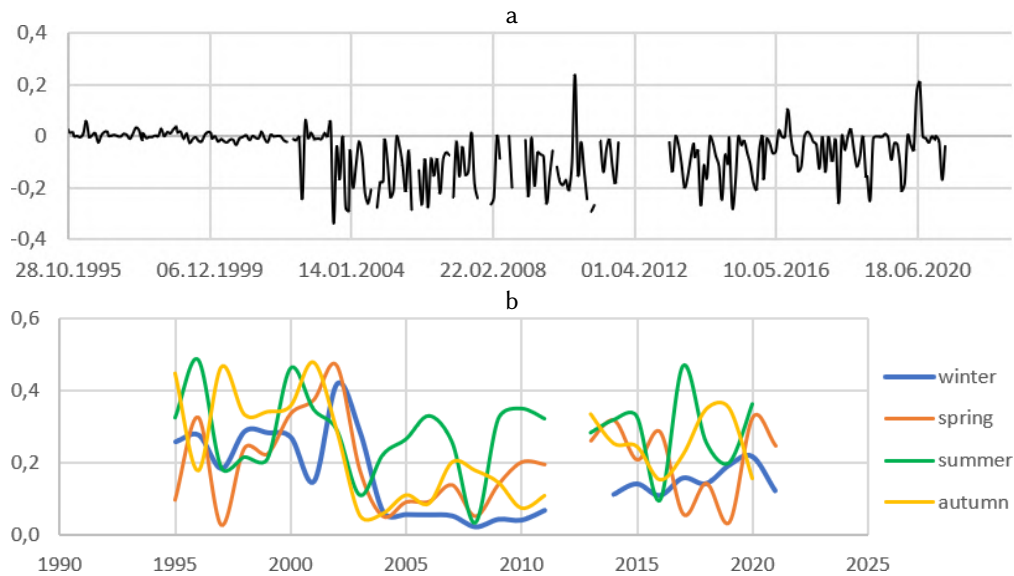


Figure 4: Time series according to Landsat-5/8 data for 1995–2021: a — RRI_32d for the test site; b — moving averages of seasonal NDVI_32d ($w = 3$).

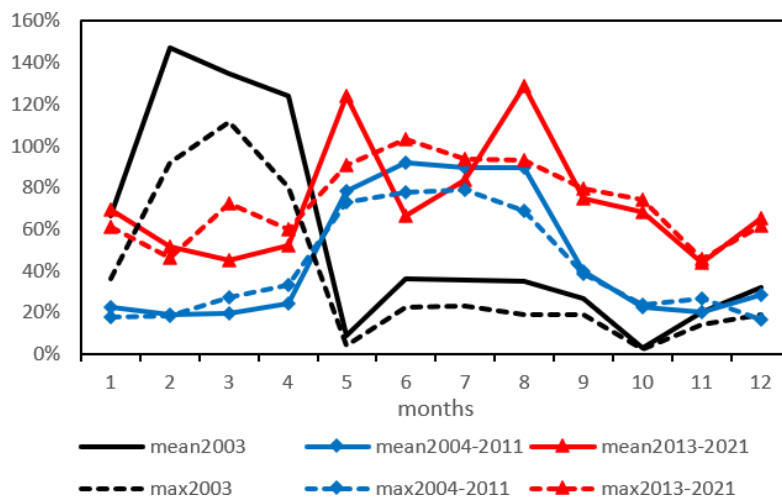


Figure 5: Seasonal changes in the SRI stand recovery index after the 2003 fire relative to the pre-fire NDVI values (1995–2002).

with dashed lines. For clarity, the graph also presents the SRI indices for the 2003 season. The graph shows a significant drop in the SRI index to 9% of the average pre-fire level (4% of the maximum) in May 2003, immediately after the fire. Already in the summer of 2003, there is a partial recovery of the index to 36% (20%). But in the autumn period, the figure drops to 2% of the pre-fire level at the same time of the year. After a fire in the interval 2004–2011 the index is recovering in summer to the level of 90% (80%), in winter – to 18–28% (16–27%). In the interval 2013–2021 index recovery in summer time is 67–130% (90–103%), in winter time – 45–70% (46–72%). As you can see from the graphs in Figure 5 and the figures shown, the average values vary significantly, while the maximum values are more stable.

6. Conclusion

To assess the degree of reforestation after the 2003 fire, a comparison was made of the polarimetric decomposition parameters, classification results, and long-term changes in seasonal fluctuations in the NDVI index in the test and control forest plots.

Comparative analysis of the parameters of the polarimetric decomposition $H - A - \alpha$ of the test and control sites showed that in 2017–2019. (14–16 years of recovery) in the test site and the field the surface type of scattering dominates, in the forest area – volume scattering. The presence of undergrowth is reflected in a higher entropy H and lower anisotropy A in comparison with the corresponding field parameters, which indicates an increase in the role of secondary types of scattering (volumetric). To assess the degree of forest regeneration, the FVC indices were calculated according to NDVI and their analogs fvcP for the parameters $H - A - \alpha$ in April 2018 FVC is 29%, fvcP for α , H and A are equal to 24, 33 and 53% respectively. Indicators are sensitive to changes in the state of polygons.

The results of the Cloude – Pottier classification showed a significant difference in the distribution of the three main types of dispersion over the area of undergrowth and healthy forest.

On average, for 2017–2019, for the test area, volume scattering and multiple reflection dominate at 21.3% and 0.2% of the territory, for the forest — by 77.7% and 19%, respectively. To confirm the results, a vegetation mask was built using a high-resolution image, which showed the presence of pine on 03/04/2018 on 38.06% of the test site and on 98.56% of the forest area. According to polarimetry data, on 04/18/2018, the presence of vegetation was determined at 31.36% and 98.29% (total volumetric and multiple scattering) of the respective territories.

As a result of the study of long-term changes in seasonal fluctuations of the NDVI for the period 1995–2021. differences in multi-season tracks, speed and recovery time of post-fire NDVI values to the level of the pre-fire period and the level of reference areas of the neighboring forest unaffected by the fire were revealed. On the test site, over the first 10 years, summer indices are restored to 80–90%, winter to 20–30%. By 2021, summer indices have been restored to 100–130%, winter to 45–70%.

The combination of radar polarimetry and optical data allows a better understanding of the process of forest restoration in general and its components.

Acknowledgments

The authors would like to thank Japanese aerospace agency (JAXA) for ALOS-2 PALSAR-2 data granted under ALOS-2 RA6 (PI-3092). The research was carried out within the state assignment of Ministry of Science and Higher Education of the Russian Federation and partially supported by the Russian Foundation for Basic Research (grant No. 18-47-030001-r_a).

References

- [1] The national project Ecology. Available at: <https://ecologyofrussia.ru/proekt/sohranenie-lesov> (accessed 08/03/2018).
- [2] Chernov M.V., Khanov S.M. Methodological approaches to the use of Earth remote sensing data in the implementation of state monitoring of forest reproduction // Proceedings of the St. Petersburg Scientific Research Institute of Forestry. 2018. No. 3–4. P. 66–76.
- [3] On the approval of the procedure for state monitoring of forest reproduction: Order of the Ministry of Natural Resources of Russia dated 19.02.2015 No. 59. Moscow: Registered in the Ministry of Justice of Russia 12.10.2015 No. 39300 // ConsultantPlus: Official Website of the ConsultantPlus Company / ConsultantPlus Company. Available at: http://www.consultant.ru/document/cons_doc_LAW_185523 (accessed 08/03/2018).
- [4] Karpov A.A., Bogdanov A.P., Pirtskhalava-Karpova N.R., Demina N.A. The use of remote sensing data for monitoring reforestation in boreal forests // News of the St. Petersburg Forestry Academy. 2019. No. 229. P. 23–43.
- [5] State report on the state and protection of the environment of the Republic of Buryatia for 2003–2016.
- [6] Forest plan of the Republic of Buryatia. Ulan-Ude, 2018.
- [7] Dorzhiev Ts.Z., Bao Y., Badmaeva E.N., Batsaikhan V., Urbazhev Ch.B., Yushan Y. Forest fires in the Republic of Buryatia for 2002–2016 // Nature of Inner Asia. 2017. No. 3(4). P. 23–35.

- [8] Evdokimenko M.D. Geography and causes of fires in the Baikal forests // News of Higher Educational Institutions. Forest Journal. 2013.
- [9] Borisova T.A. Causes of forest fires in Buryatia: Causes and consequences // Vestnik VSU. Series: Geography, Geoecology. 2017. No. 2. P. 78–84.
- [10] Rymorev M.V., Altayev A.A. Reforestation in the Republic of Buryatia // Modern Technologies in Agronomy, Forestry and Methods for Regulating Soil Fertility. Materials of the International Scientific-Practical Conference Eedicated to the 65th Anniversary of the Agronomic Faculty of the Belarusian State Agricultural Academy. BGSKhA im. V.R. Filippov, 2017.
- [11] Landsat 8 Collection 1 Tier 1 32-Day NDVI Composite. Available at: https://developers.google.com/earth-engine/datasets/catalog/LANDSAT_LC08_C01_T1_32DAY_NDVI (accessed 08/22/2021).
- [12] Manual of remote sensing. Vol. 2. Principles and applications of imaging radar / R.A. Ryerson (Ed.). USA: Wiley, 1998. 865 p.
- [13] Cloude S.R., Pottier E. An entropy-based classification scheme for land applications of polarimetric SAR // IEEE Trans GRS. 1997. Vol. 35(1). P. 68–78.
- [14] Cloude S.R., Pottier E. A review of target decomposition theorems in radar polarimetry // IEEE Transactions on Geoscience and Remote Sensing. 1996. Vol. 34. No. 2. P. 498–518.
- [15] Chu T., Guo X., Takeda K. Remote sensing approach to detect post-fire vegetation regrowth in Siberian boreal larch forest // Ecological Indicators. 2016. No. 62. P. 32–46.
- [16] Yi K., Tani H., Zhang J., Guo M., Wang X., Zhong G. Long-term satellite detection of post-fire vegetation trends in boreal forests of China // Remote Sensing. 2013. No. 5(12). P. 6938–6957.